

Cite this: *Chem. Sci.*, 2024, 15, 11367

All publication charges for this article have been paid for by the Royal Society of Chemistry

# Blue light emission enhancement and robust pressure resistance of gallium oxide nanocrystals†

Zongqing Jin,<sup>a</sup> Pengfei Lv,<sup>a</sup> Yifan Xu,<sup>a</sup> Yongguang Li,<sup>b</sup> Qingfeng Dong,<sup>c</sup> Guanjun Xiao<sup>\*,a</sup> and Bo Zou<sup>a</sup>

Exploration of pressure-resistant materials largely facilitates their operation under extreme conditions where a stable structure and properties are highly desirable. However, under extreme conditions, such as a high pressure over 30.0 GPa, fluorescence quenching generally occurs in most materials. Herein, pressure-induced emission enhancement (PIEE) by a factor of 4.2 is found in Ga<sub>2</sub>O<sub>3</sub> nanocrystals (NCs), a fourth-generation ultrawide bandgap semiconductor. This is mainly attributed to pressure optimizing the intrinsic lattice defects of the Ga<sub>2</sub>O<sub>3</sub> nanocrystals, which was further confirmed by first-principles calculations. Note that the bright blue emission could be stabilized even up to a high pressure of 30.6 GPa, which is of great significance in the essential components of white light. Notably, after releasing the pressure to ambient conditions, the emission of the Ga<sub>2</sub>O<sub>3</sub> nanocrystals can completely recover, even after undergoing multiple repeated pressurizations. In addition to stable optical properties, synchrotron radiation shows that the Ga<sub>2</sub>O<sub>3</sub> nanocrystals remain in the cubic structure described by space group *Fd3m* upon compression, demonstrating the structural stability of the Ga<sub>2</sub>O<sub>3</sub> nanocrystals under high pressure. This study pays the way for the application of oxide nanomaterials in pressure anti-counterfeiting and pressure information memory devices.

Received 3rd April 2024  
Accepted 9th June 2024

DOI: 10.1039/d4sc02204a

rsc.li/chemical-science

## Introduction

Luminescent materials in response to environmental stimuli have drawn increasing research interest for their potential applications in information storage, optoelectronic devices and sensors.<sup>1–5</sup> Over the past few decades, various kinds of luminescent materials, including halide perovskites, organic molecules and quantum dots, have shown interesting pressure-induced photoluminescence (PL) changes.<sup>6–9</sup> For example, pressure-induced emission (PIE) and piezochromism were found in the compelling materials of Cs<sub>4</sub>PbBr<sub>6</sub> nanocrystals (NCs) and Rb<sub>2</sub>TeCl<sub>6</sub> microcrystals (MCs), respectively.<sup>10–12</sup> However, above-mentioned materials usually suffered from PL quenching under extremely high pressures of over 30 GPa,<sup>5–7,10</sup> resulting from the non-radiative contribution. In addition, few materials could retain their initial optical properties after full pressure release, which greatly limits their practical

applications. Therefore, there is an urgent need to explore materials that can keep their intense PL intensity under high pressure.

Compared to the above-mentioned materials, semiconductor oxides have shown relative stability in response to external pressure.<sup>13–15</sup> At the turn of the century, Jiang *et al.* performed a study of the effects of pressure on ZnO NCs, revealing that the ZnO NCs maintained structural stability over 15.0 GPa, while it was only 9.9 GPa for bulk ZnO. This finding sparked interest in the pressure-related stabilization of semiconductor oxide NCs.<sup>13</sup> Wang *et al.* further reported that β-Ga<sub>2</sub>O<sub>3</sub> NCs exhibited no structural transition after reaching 16.4 GPa.<sup>14</sup> The optical properties of the oxide NCs also have attracted research interest because of their unique defect emission mechanism. Oxygen vacancies in nanocrystalline oxides are known to be common and prevalent defects, acting as emission centers and radiative traps in luminescence processes.<sup>16–21</sup> They can also form defect levels in the band gap and contribute to mid-gap luminescence.<sup>16</sup> However, few studies have focused on the pressure-dependent change in their optical properties. Considering the structural stability of the semiconductor oxides under pressure, it is imperative to study their optical properties that can glow sustainably under pressure.

Herein, we conducted a systematic investigation on the optical properties and crystal structure of γ-Ga<sub>2</sub>O<sub>3</sub> NCs under high pressure. We observed a 4.2-fold increase in the PL

<sup>a</sup>State Key Laboratory of Superhard Materials, College of Physics, Jilin University, Changchun 130012, China. E-mail: xguanjun@jlu.edu.cn

<sup>b</sup>Key Laboratory of Organosilicon Chemistry and Material Technology Ministry of Education, College of Material, Chemistry and Chemical Engineering, Hangzhou Normal University, Hangzhou 311121, China

<sup>c</sup>State Key Laboratory of Supermolecular Structure and Materials, College of Chemistry, Jilin University, Changchun 130012, China

† Electronic supplementary information (ESI) available. See DOI: <https://doi.org/10.1039/d4sc02204a>



intensity of Ga<sub>2</sub>O<sub>3</sub> NCs under pressure. This phenomenon was attributed to pressure-induced optimized lattice defects. First-principles calculations showed the defect reduction and lattice optimization of the Ga<sub>2</sub>O<sub>3</sub> NCs under pressure are related to a decrease in oxygen vacancy formation energy, which corresponds to a resulting increase in the PL intensity. Notably, even at an elevated pressure of 30.6 GPa, the PL intensity of the Ga<sub>2</sub>O<sub>3</sub> NCs remained stronger than that observed under normal conditions. Furthermore, our results from high-pressure absorption spectra and ADXRD revealed that the band gap and crystal structure of the Ga<sub>2</sub>O<sub>3</sub> NCs exhibited remarkable stability and exceptional resistance to high pressure, respectively. Because of their outstanding stability and super “pressure resistance,” the Ga<sub>2</sub>O<sub>3</sub> NCs can potentially enable multiple copying functions under pressure, thereby enhancing device longevity and positioning themselves as promising candidates for next-generation stable ultra-pressure-resistant luminescent materials.

## Results and discussion

The Ga<sub>2</sub>O<sub>3</sub> NCs were synthesized by a modified colloidal hot injection experiment.<sup>18–22</sup> Fig. 1a shows the morphology and microstructure of the Ga<sub>2</sub>O<sub>3</sub> NCs, characterized by transmission electron microscopy (TEM) and high-resolution transmission electron microscopy (HRTEM). It is observed that synthesized

Ga<sub>2</sub>O<sub>3</sub> NCs are homogeneous nanoparticles with a well mono-dispersed spherical shape. The inset in Fig. 1a shows a Gaussian fit of the Ga<sub>2</sub>O<sub>3</sub> NCs with an average diameter of approximately 3.2 nm. The Ga<sub>2</sub>O<sub>3</sub> NCs exhibit a broad blue PL emission at an excitation wavelength of 355 nm (Fig. 1b). The biexponential equation fitted the results well (Fig. S1 ESI†), indicating that the average fluorescence lifetime of the Ga<sub>2</sub>O<sub>3</sub> NCs is approximately 2.5 ns. The photoluminescence quantum yield (PLQY) is measured to be about 16% for the Ga<sub>2</sub>O<sub>3</sub> NCs. We modified XRD patterns with the corresponding refinement and residual by GSAS. In terms of the peak width of (311) planes, the particle size is estimated to be about 3.07 nm, as determined by the Scherrer formula.<sup>23</sup> XRD analysis and structural simulations show that the synthesized Ga<sub>2</sub>O<sub>3</sub> NCs belong to the γ-Ga<sub>2</sub>O<sub>3</sub> cubic structure described by space group *Fd3m* (Fig. 1c and d).<sup>18,21,24</sup>

We further investigated the optical properties of the Ga<sub>2</sub>O<sub>3</sub> NCs under high pressure. Experiments were performed using silicone oil as a pressure medium, which remains quasi-hydrostatic up to 4 GPa.<sup>25</sup> For more details on the experiments, see ESI.† As shown in Fig. 2a, the PL intensity of the Ga<sub>2</sub>O<sub>3</sub> NCs increased significantly and reached its highest intensity at 6.0 GPa, which was 4.2 times the initial intensity. Comparative experiments with commercial bulk Ga<sub>2</sub>O<sub>3</sub> demonstrated that bulk Ga<sub>2</sub>O<sub>3</sub> did not show the PIEE phenomenon. The luminescence stability of the Ga<sub>2</sub>O<sub>3</sub> NCs is

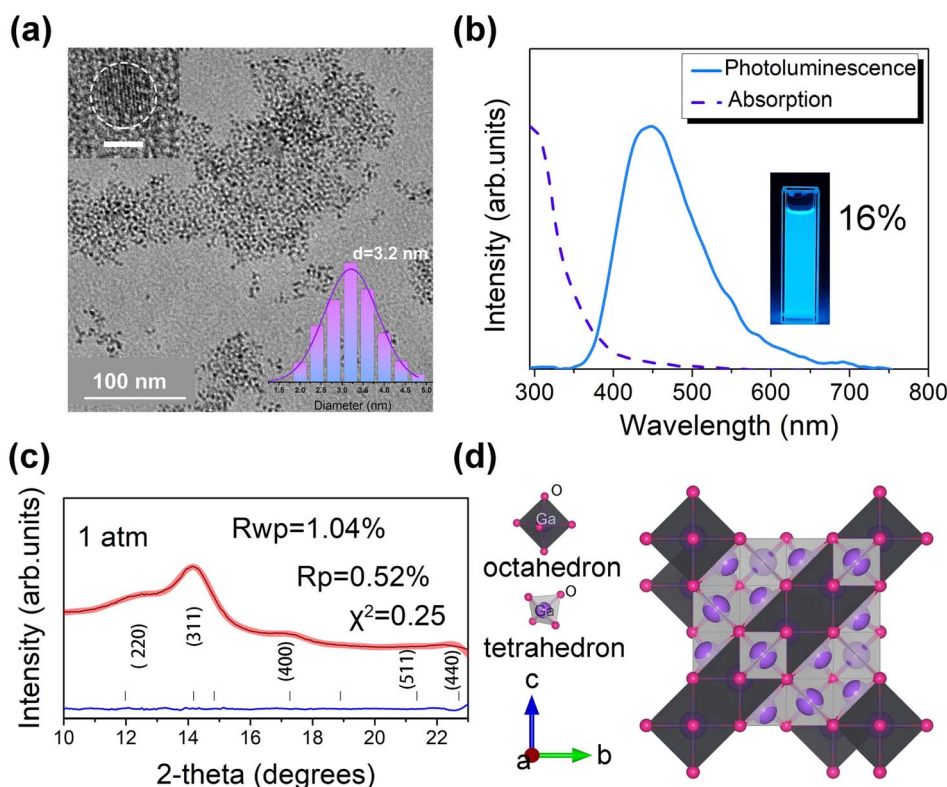


Fig. 1 (a) TEM image of the Ga<sub>2</sub>O<sub>3</sub> NCs. The top inset shows the high-resolution TEM image whose scale bar is 5 nm. The bottom inset shows the corresponding size distribution of as-prepared Ga<sub>2</sub>O<sub>3</sub> NCs. (b) Steady-state absorption spectra and PL spectra excited by 355 nm monochromatic light. The inset shows a fluorescence photograph under 365 nm excitation. (c) Rietveld refinements of the Ga<sub>2</sub>O<sub>3</sub> NCs at 1 atm. (d) Schematic of the cubic crystal spinel structure of the Ga<sub>2</sub>O<sub>3</sub> NCs.



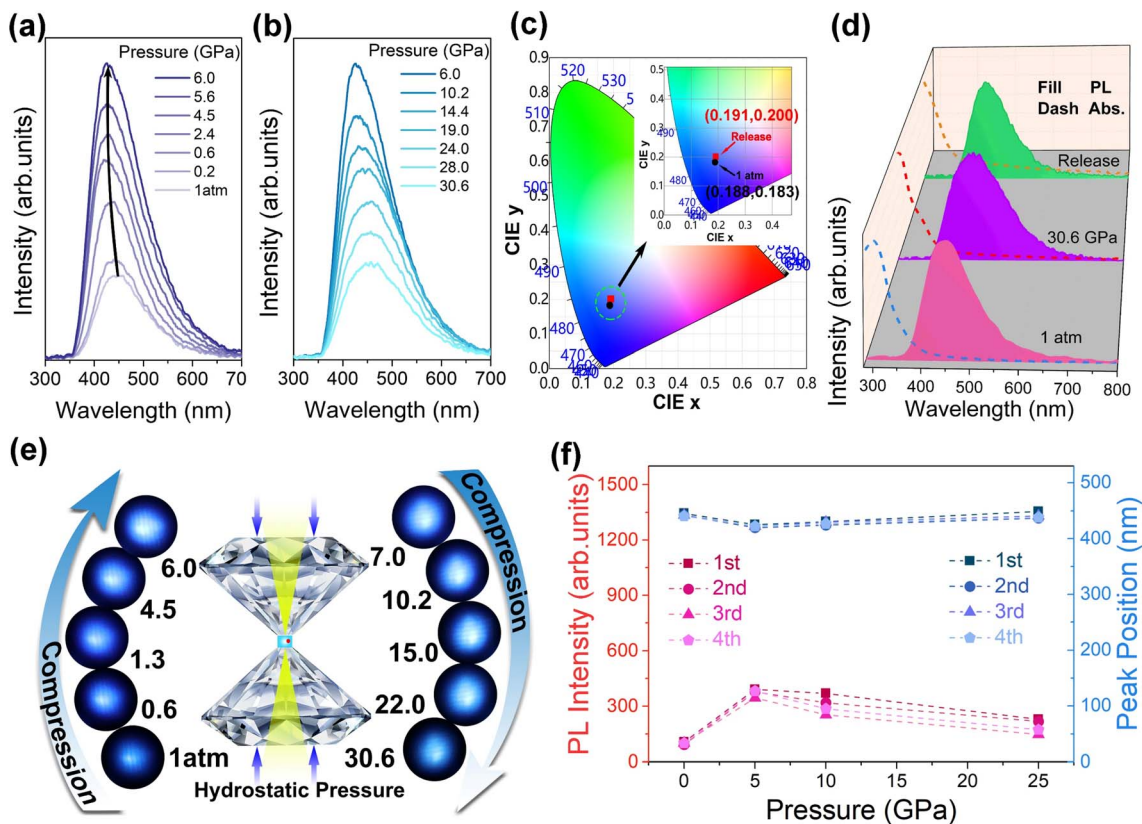


Fig. 2 (a) and (b) PL spectra of the  $\text{Ga}_2\text{O}_3$  NCs under high pressure. (c) Chromaticity coordinate diagram where the green dashed line shows a region of ambient pressure and release for the selected chromaticity values of the  $\text{Ga}_2\text{O}_3$  NCs. (d) Absorption and emission spectra of the  $\text{Ga}_2\text{O}_3$  NCs at 1 atm pressure, 30.6 GPa and decompression. (e) PL micrographs of the  $\text{Ga}_2\text{O}_3$  NCs upon compression under 355 nm photo-excitation. (f) Changes in peak position and intensity of repeated compression emission from the  $\text{Ga}_2\text{O}_3$  NCs. (The error of all pressures measured in the experiments is  $\pm 0.1$  GPa.)

better than that of the bulk counterpart, as shown Fig. S2.† Note that, although the PL intensity of the  $\text{Ga}_2\text{O}_3$  NCs started to weaken slowly when the pressure exceeded 6.0 GPa, the emission of the  $\text{Ga}_2\text{O}_3$  NCs still stronger than that under normal pressure up to 30.6 GPa (Fig. 2b). Meanwhile, the PL peak position of the  $\text{Ga}_2\text{O}_3$  NCs remained almost unchanged under high pressure, which highlights the stability and super “pressure resistance” of the  $\text{Ga}_2\text{O}_3$  NCs. Pressure-dependent colorimetry coordinates (CIE) indicate that the fluorescent color of the  $\text{Ga}_2\text{O}_3$  NCs is less affected by pressure, indicating that the optical properties of the  $\text{Ga}_2\text{O}_3$  NCs show excellent stability under pressure (Fig. 2c). In Fig. 2d, the absorption and emission spectra of the  $\text{Ga}_2\text{O}_3$  NCs are almost identical under 1 atm, 30.6 GPa and release. The optical microscope images of the  $\text{Ga}_2\text{O}_3$  NCs *versus* pressure in a diamond anvil cell chamber clearly illustrate the variation in PL brightness (Fig. 2e). We also designed repeated high-pressure experiments for the synthesized  $\text{Ga}_2\text{O}_3$  NCs to further demonstrate the “pressure resistance” of the  $\text{Ga}_2\text{O}_3$  NCs under high pressure (Fig. S3†). As shown in Fig. 2f, the changes in emission intensity and peak position of the  $\text{Ga}_2\text{O}_3$  NCs remained consistent, with good stability and reproducibility throughout four compression cycles. When the pressure was fully released to ambient conditions, the sample almost reverted to the initial PL intensity and color (Fig. S4†). The reversibility of the  $\text{Ga}_2\text{O}_3$  NCs

under pressure can effectively improve the material reuse life of a pressure sensor (Fig. S5†).

An *in situ* high-pressure cycle experiment on ultraviolet-visible absorption spectra was performed to characterize the bandgap evolution in the  $\text{Ga}_2\text{O}_3$  NCs (Fig. 3a and S6†). It is observed that the 355 nm absorption edge of the  $\text{Ga}_2\text{O}_3$  NCs underwent only a minor redshift during pressurization. The alteration in the band gap was estimated using the Tauc plot fitted with the absorption spectrum. The band structure and density of state of the  $\text{Ga}_2\text{O}_3$  NCs were calculated using first-principles density functional theory (DFT) calculations, which confirmed that the  $\text{Ga}_2\text{O}_3$  NCs belong to the direct bandgap (Fig. 3b).<sup>24</sup> Fig. 3b shows that DFT underestimates the band-gap energy, which is a typical feature of DFT calculation.<sup>26</sup> According to Fig. 3c and S7,† the  $\text{Ga}_2\text{O}_3$  NCs exhibited a decrease in band gap when compressed from ambient conditions to 4.0 GPa, followed by a slow decrease. It is found that there is only a marginal overall variation of approximately 0.2 eV in absorbed and emitted energy during compression. After the pressure was fully released, absorbed energy and Stokes displacement remained nearly unchanged compared to their initial values, indicating structural reversibility (Fig. 3c). The relationship between the stable optical properties and structure of the  $\text{Ga}_2\text{O}_3$  NCs was investigated by high-pressure ADXRD experiments.<sup>10,27–30</sup> Experimental results from ADXRD showed



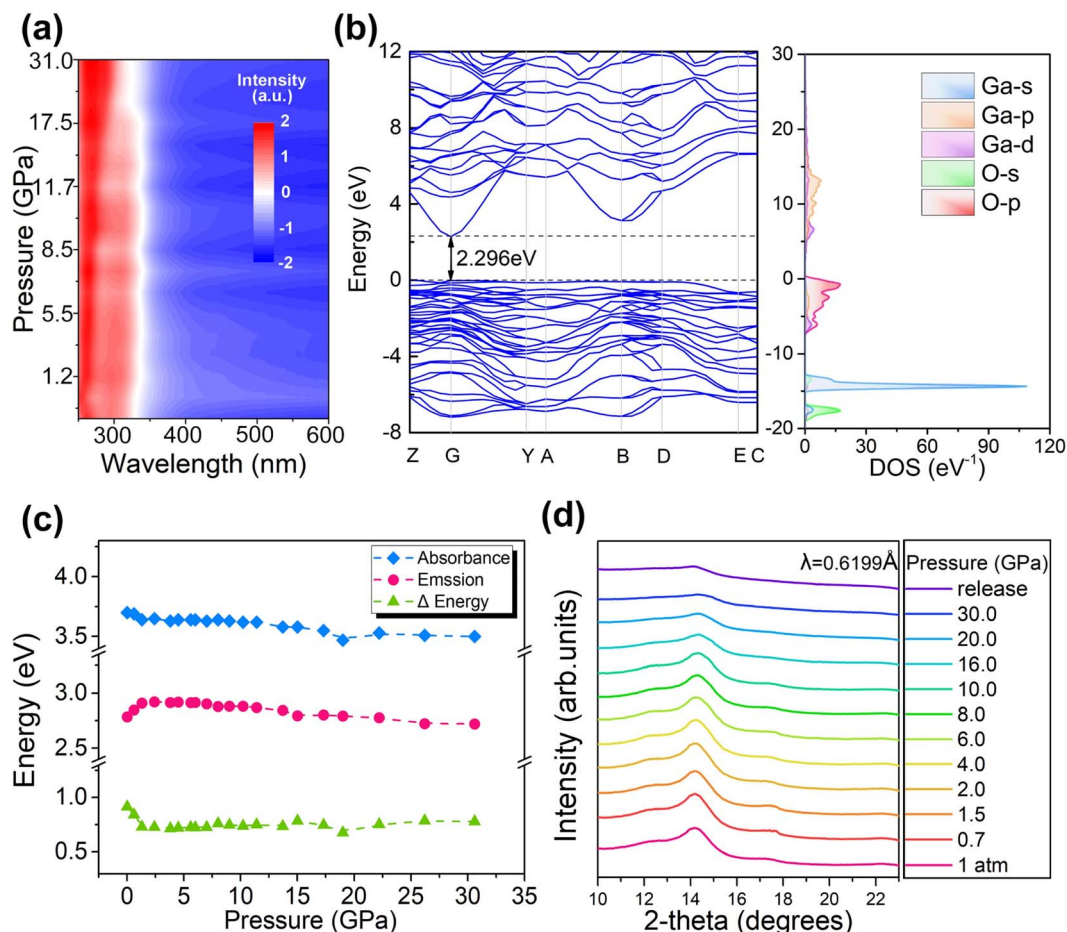


Fig. 3 (a) Pressure-dependent optical absorption spectra of the Ga<sub>2</sub>O<sub>3</sub> NCs. (b) DFT-calculated band structure and projected density of states of Ga<sub>2</sub>O<sub>3</sub> NCs under ambient conditions. (c) Absorption and emission energies of the Ga<sub>2</sub>O<sub>3</sub> NCs upon compression. (d) High-pressure ADXRD pattern for the Ga<sub>2</sub>O<sub>3</sub> NCs.

that the Ga<sub>2</sub>O<sub>3</sub> NCs maintained a stable phase structure as the pressure reached 30.6 GPa (Fig. 3d). We carried out a transmission electron microscope (TEM) test of samples after the restoration of environmental conditions. It was found that the morphology of the samples under atmospheric pressure and after releasing pressure are nanoparticles without obvious changes (Fig. S8†). Therefore, all of the optical properties, structure and morphology of the Ga<sub>2</sub>O<sub>3</sub> NCs can remain stable after pressure treatment. The volume data was fitted with a third-order Birch–Murnaghan equation of state:<sup>31–33</sup>

$$P(V) = \frac{3B_0}{2} \left[ \left( \frac{V_0}{V} \right)^{\frac{7}{3}} - \left( \frac{V_0}{V} \right)^{\frac{5}{3}} \right] \left\{ 1 + \frac{3}{4} (B'_0 - 4) \left[ \left( \frac{V_0}{V} \right)^{\frac{2}{3}} - 1 \right] \right\},$$

where  $V_0$  is the volume at zero pressure,  $B_0$  is the bulk modulus at ambient pressure, and  $B'_0$  is a parameter for the pressure derivative. The fitting of the Birch–Murnaghan equation

indicated that the isothermal bulk modulus  $B_0$  for the Ga<sub>2</sub>O<sub>3</sub> NCs was estimated as 137.34 GPa, much higher than that (85.9 GPa) of the bulk counterpart<sup>34</sup> (Fig. S9†). Materials showing higher bulk modulus are more difficult to compress, which further illustrates the stability of the Ga<sub>2</sub>O<sub>3</sub> NCs.

The cause of the luminescence in Ga<sub>2</sub>O<sub>3</sub> is generally believed to be acceptor–donor pair (DAP) recombination, and oxygen vacancy defects are crucial in DAP recombination.<sup>18,19,27,35–37</sup> For the DAP recombination model, the energy ( $E$ ) of the emitted photon depends on the distance ( $r$ ) between donor and acceptor sites and can be expressed by the following equation:

$$E(r) = E_g - (E_A + E_D) + \frac{e^2}{4\pi\epsilon_0\epsilon_r r^2}, \quad (1)$$

where the first term  $E_g$  is the band gap energy of Ga<sub>2</sub>O<sub>3</sub>; second and third terms  $E_A$  and  $E_D$  are the binding energies of the acceptor and donor; and the fourth term is the coulombic energy between the acceptor and donor, where  $r$  is the distance between the acceptor and donor.

We analyzed the behavior of the oxygen vacancy defects under pressure by simulating the formation energy of the oxygen vacancy defects at different pressures,<sup>18,19,38</sup> which can be represented by following equations:



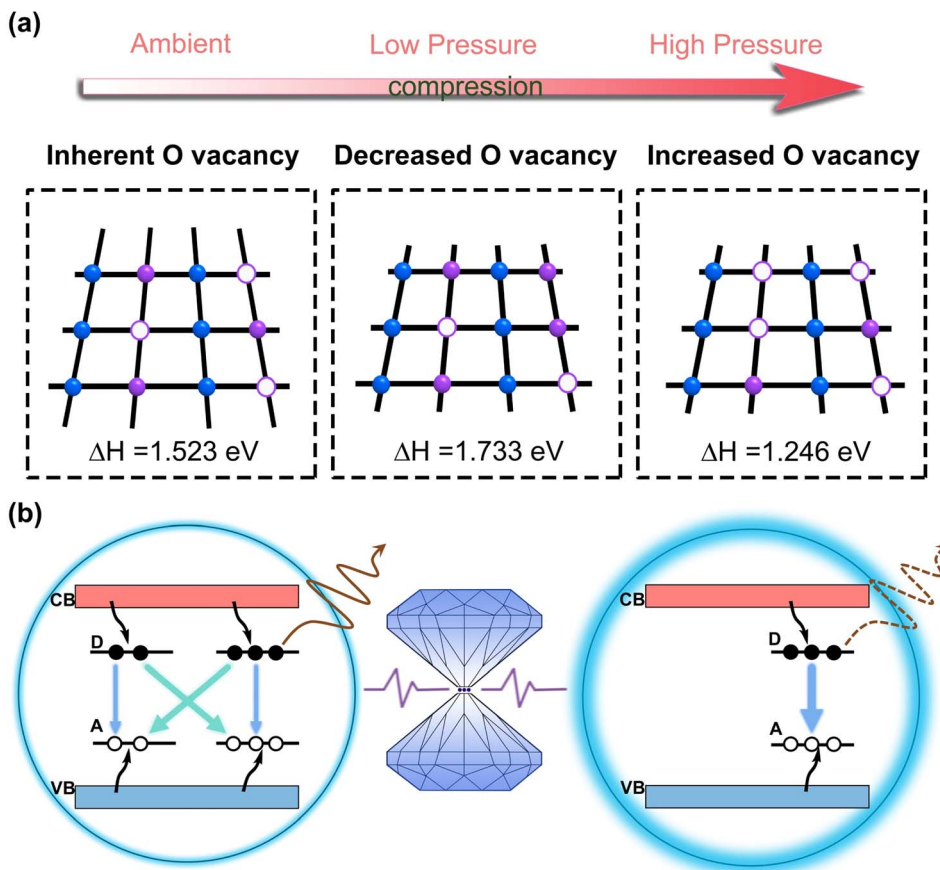


Fig. 4 (a) Schematic representation of the mechanism of oxygen-vacancy-induced defect luminescence and pressure-induced emission enhancement. (Blue dots are Ga atoms, purple dots are O atoms, and purple circles are O vacancies.) (b) Schematic of the DAP model with the binding energy of acceptor and donor.

$$\Delta H = E_{\text{O}} - E_{\text{P}} + \mu_{\text{O}} \quad (2)$$

$$\mu_{\text{O}} = \frac{(E_{\text{P}} - E_{\text{Ga}})}{32}, \quad (3)$$

where  $E_{\text{O}}$  is the energy of containing the oxygen vacancy defects;  $E_{\text{P}}$  is the energy of completeness;  $E_{\text{Ga}}$  is the energy of containing only Ga atoms;  $\mu_{\text{O}}$  is the chemical potential of oxygen in  $\text{Ga}_2\text{O}_3$  NCs; and  $\Delta H$  is the energy of formation of the oxygen vacancy defects.

The oxygen vacancy formation energy ( $\Delta H$ ) of the  $\text{Ga}_2\text{O}_3$  NCs was calculated at atmospheric pressure, 1.5 GPa, 3.0 GPa and 4.5 GPa (Fig. S10†). The results show that  $\Delta H$  increases in the low-pressure region (<1.5 GPa), resulting in the suppression of oxygen vacancy defect formation. This contributes to a certain degree of lattice optimization of the  $\text{Ga}_2\text{O}_3$  NCs.<sup>27,38–40</sup> In the high-pressure region (>1.5 GPa), because of the excessive degree of lattice distortion in the  $\text{Ga}_2\text{O}_3$  NCs,  $\Delta H$  decreases. The proposed mechanism regarding the pressure increase of the oxygen vacancies is fully coherent with the broadening of XRD peaks, as shown in Fig. 3d, and decrease in signal intensity, which is probably due to pressure-driven disorder in the crystal structure.<sup>41</sup> This trend promotes an increase in defects, giving rise to a slow decrease in emission. The suppression of oxygen vacancy defect formation will lead to a decrease in the distance

( $r$ ) between the acceptor and donor in the DAP complex,<sup>27,38</sup> and hence a shift in DAP emission towards higher energy (Fig. 4a).<sup>19,20,36,37</sup> This finding further supports the blueshift observed in the  $\text{Ga}_2\text{O}_3$  NCs under low-pressure conditions. Furthermore, defects in crystals exhibit two primary types of behavior: (1) non-radiative leaps and (2) DAP luminescence.<sup>18,19,27,35,36</sup> The majority of the oxygen vacancy defects in the  $\text{Ga}_2\text{O}_3$  NCs participate in non-radiative transitions, while only a small proportion are involved in DAP complexes.<sup>27</sup> Combining theoretical calculations, a reasonable conclusion is that the non-radiative leaps in the  $\text{Ga}_2\text{O}_3$  NCs are suppressed under pressure, which eventually leads to the enhancement in emission of the  $\text{Ga}_2\text{O}_3$  NCs.<sup>27</sup>

## Conclusions

Based on the well-established theory of oxygen-vacancy point-defect-induced emission in the  $\text{Ga}_2\text{O}_3$  NCs, we devised a high-pressure engineering approach and successfully achieved remarkable PIEE, as well as significant repeated compression-stable emission of the  $\text{Ga}_2\text{O}_3$  NCs. During the compression process, the blue emission intensity of the  $\text{Ga}_2\text{O}_3$  NCs is enhanced by approximately 4.2 times, which is attributed to pressure optimizing the intrinsic lattice defects of the  $\text{Ga}_2\text{O}_3$



NCs. Note that the bright blue emission could be stabilized even up to a high pressure of 30.6 GPa. In contrast, bulk materials exhibited an opposite trend with reduced emission intensity upon compression. High-pressure ADXRD data further confirmed that the Ga<sub>2</sub>O<sub>3</sub> NCs do not undergo a structural phase transition because of their inherent stability and resistance to pressure effects. Our study elucidated the correlation between the structure and properties of the Ga<sub>2</sub>O<sub>3</sub> NCs, which aligned with the general theory of oxygen-vacancy point-defect-induced emission and offered valuable insights for potential applications in third-generation oxide semiconductors and optical pressure sensor materials.

## Data availability

The data that support the findings of this study are available in the ESI† of this article.

## Author contributions

G. X. and B. Z. designed the experiments. Z. J. and Y. X., performed the experiments and analyzed data. P. L., Y. L. and D. Q. performed partial experiments and calculations. Z. J., P. L., G. X. and B. Z. wrote the manuscript.

## Conflicts of interest

There are no conflicts to declare.

## Acknowledgements

This work is supported by the National Key R&D Program of China (2023YFA1406200), Jilin Provincial Science & Technology Development Program (20220101002JC), National Science Foundation of China (12174144), Zhejiang Provincial Natural Science Foundation of China (LR22B010001), Graduate Innovation Fund of Jilin University (2023CX040; 2023CX185) and Fundamental Research Funds for the Central Universities. This work was mainly performed at BL15U1 at the Shanghai Synchrotron Radiation Facility (SSRF).

## Notes and references

- 1 S. Kim, S. J. Yoon and S. Y. Park, Highly Fluorescent Chameleon Nanoparticles and Polymer Films, Multicomponent Organic Systems that Combine FRET and Photochromic Switching, *J. Am. Chem. Soc.*, 2012, **134**, 12091–12097.
- 2 D. H. Kim, A. D'Aléo, X. K. Chen, A. D. S. Sandanayaka, D. Yao, L. Zhao, T. Komino, E. Zaborova, G. Canard, Y. Tsuchiya, E. Choi, J. W. Wu, F. Fages, J. L. Brédas, J. C. Ribierre and C. Adachi, High-efficiency electroluminescence and amplified spontaneous emission from a thermally activated delayed fluorescent near-infrared emitter, *Nat. Photonics*, 2018, **12**, 98–104.
- 3 Y. Wang, X. Tan, Y. M. Zhang, S. Zhu, I. Zhang, B. Yu, K. Wang, B. Yang, M. Li, B. Zou and S. X. A. Zhang, Dynamic behavior of molecular switches in crystal under pressure and its reflection on tactile sensing, *J. Am. Chem. Soc.*, 2015, **137**, 931–939.
- 4 Y. Zhao, N. Li, C. Xu, Y. Li, H. Zhu, P. Zhu, X. Wang and W. Yang, Abnormal pressure-Induced photoluminescence enhancement and phase decomposition in pyrochlore La<sub>2</sub>Sn<sub>2</sub>O<sub>7</sub>, *Adv. Mater.*, 2017, **29**, 1701513.
- 5 Q. Lou, X. Yang, K. Liu, Z. Ding, J. Qin, Y. Li, C. Lv, Y. Shang, Y. Zhang, Z. Zhang, J. Zang, L. Dong and C. X. Shan, Pressure-induced photoluminescence enhancement and ambient retention in confined carbon dots, *Nano Res.*, 2022, **15**, 2545–2551.
- 6 Z. Chi, X. Zhang, B. Xu, X. Zhou, C. Ma, Y. Zhang, S. Liu and J. Xu, Recent advances in organic mechanofluorochromic materials, *Chem. Soc. Rev.*, 2012, **41**, 3878–3896.
- 7 N. Chauvin, A. Mavel, G. Patriarche, B. Masenelli, M. Gendry and D. Machon, Pressure-dependent photoluminescence study of wurtzite InP nanowires, *Nano Lett.*, 2016, **16**, 2926–2930.
- 8 G. Xiao, X. Yang, X. Zhang, K. Wang, X. Huang, Z. Ding, Y. Ma, G. Zou and B. Zou, A protocol to fabricate nanostructured new phase: B31-type MnS synthesized under high pressure, *J. Am. Chem. Soc.*, 2015, **137**, 10297–10303.
- 9 G. Xiao, Y. Wang, D. Han, K. Li, X. Feng, P. Lv, K. Wang, L. Liu, S. A. T. Redfern and B. Zou, Pressure-induced large emission enhancements of cadmium selenide nanocrystals, *J. Am. Chem. Soc.*, 2018, **140**, 13970–13975.
- 10 Z. Ma, Z. Liu, S. Lu, L. Wang, X. Feng, D. Yang, K. Wang, G. Xiao, L. Zhang, S. A. T. Redfern and B. Zou, Pressure-induced emission of cesium lead halide perovskite nanocrystals, *Nat. Commun.*, 2018, **9**, 4506.
- 11 W. Zhao, Z. Ma, Y. Shi, R. Fu, K. Wang, Y. Sui, G. Xiao and B. Zou, Pressure tailoring electron-phonon coupling toward enhanced yellow photoluminescence quantum yield and piezochromism, *Cell Rep. Phys. Sci.*, 2023, **4**, 101663.
- 12 Z. W. Ma, G. J. Xiao and B. Zou, Step forward to light up the future: pressure-induced emission, *Sci. Bull.*, 2023, **68**, 1588–1590.
- 13 J. Z. Jiang, J. S. Olsen, L. Gerward, D. Frost, D. Rubie and J. Peyronneau, Structural stability in nanocrystalline ZnO, *Europhys. Lett.*, 2000, **50**, 48.
- 14 H. Wang, Y. He, W. Chen, Y. W. Zeng, K. Stahl, T. Kikegawa and J. Z. Jiang, High-pressure behavior of β-Ga<sub>2</sub>O<sub>3</sub> nanocrystals, *J. Appl. Phys.*, 2010, **107**, 033520.
- 15 L. Wang, Y. Pan, Y. Ding, W. Yang, W. L. Mao, S. V. Sinogeikin, Y. Meng, G. Shen and H.-k. Mao, High-pressure induced phase transitions of Y<sub>2</sub>O<sub>3</sub> and Y<sub>2</sub>O<sub>3</sub>:Eu<sup>3+</sup>, *Appl. Phys. Lett.*, 2009, **94**, 061921.
- 16 T. Lim, S. Lee, M. Meyyappan and S. Ju, Control of semiconducting and metallic indium oxide nanowires, *ACS Nano*, 2011, **5**, 3917–3922.
- 17 T. Harwig and F. Kellendonk, Some observations on the photoluminescence of doped β-galliumsesquioxide, *J. Solid State Chem.*, 1978, **24**, 255–263.



- 18 T. Wang and P. V. Radovanovic, Size-dependent electron transfer and trapping in strongly luminescent colloidal gallium oxide nanocrystals, *J. Phys. Chem. C*, 2011, **115**, 18473–18478.
- 19 T. Wang, S. S. Farvid, M. Abulikemu and P. V. Radovanovic, Size-tunable phosphorescence in colloidal metastable  $\gamma$ -Ga<sub>2</sub>O<sub>3</sub> nanocrystals, *J. Am. Chem. Soc.*, 2010, **132**, 9250–9252.
- 20 B. Fernandes, M. Hegde, P. C. Stanish, Z. L. Mišković and P. V. Radovanovic, Photoluminescence decay dynamics in  $\gamma$ -Ga<sub>2</sub>O<sub>3</sub> nanocrystals: The role of exclusion distance at short time scales, *Chem. Phys. Lett.*, 2017, **684**, 135–140.
- 21 T. Wang and P. V. Radovanovic, In situ enhancement of the blue photoluminescence of colloidal Ga<sub>2</sub>O<sub>3</sub> nanocrystals by promotion of defect formation in reducing conditions, *Chem. Commun.*, 2011, **47**, 7161–7163.
- 22 H. Jiang, W. Zhao, R. Fu and G. Xiao, Pressure-resistance of magic-sized cadmium selenide nanocrystals, *J. Inorg. Mater.*, 2021, **36**, 502–506.
- 23 A. L. Patterson, The Scherrer formula for X-ray particle size determination, *Phys. Rev.*, 1939, **56**, 978–982.
- 24 Y. Huang, A. Gao, D. Guo, X. Lu, X. Zhang, Y. Huang, J. Yu, S. Li, P. Li and W. Tang, Fe doping-stabilized  $\gamma$ -Ga<sub>2</sub>O<sub>3</sub> thin films with a high room temperature saturation magnetic moment, *J. Mater. Chem. C*, 2020, **8**, 536–542.
- 25 D. Errandonea, Y. Meng, M. Somayazulu and D. Häusermann, Pressure-induced  $\alpha \rightarrow \omega$  transition in titanium metal: a systematic study of the effects of uniaxial stress, *Phys. B*, 2005, **355**, 116–125.
- 26 T. Ouahrani, R. M. Boufatah, M. Benaissa, Á. Morales-García, M. Badawi and D. Errandonea, Effect of intrinsic point defects on the catalytic and electronic properties of Cu<sub>2</sub>WS<sub>4</sub> single layer: Ab initio calculations, *Phys. Rev. Mater.*, 2023, **7**, 025403.
- 27 P. Lv, D. Zhao, F. Wang, Z. Ma, L. Sui, K. Yuan, K. Wang, J. Ning, G. Xiao and B. Zou, Clarifying the controversy over defect emission of I-III-VI<sub>2</sub> nanocrystals via pressure engineering, *Adv. Opt. Mater.*, 2023, **12**, 2301758.
- 28 D. Zhao, M. Cong, Z. Liu, Z. Ma, K. Wang, G. Xiao and B. Zou, Steric hindrance effects on the retention of pressure-induced emission toward scintillators, *Cell Rep. Phys. Sci.*, 2023, **4**, 101445.
- 29 Z. Ma, F. Li, D. Zhao, G. Xiao and B. Zou, Whether or not emission of Cs<sub>4</sub>PbBr<sub>6</sub> nanocrystals: High-pressure experimental evidence, *CCS Chem.*, 2020, **2**, 71–80.
- 30 F. Bai, K. Bian, X. Huang, Z. Wang and H. Fan, Pressure induced nanoparticle phase behavior, property, and applications, *Chem. Rev.*, 2019, **119**, 7673–7717.
- 31 F. Birch, Finite elastic strain of cubic crystals, *Phys. Rev.*, 1947, **71**, 809–824.
- 32 Y. Shi, Y. Fu, Z. Ma, D. Zhao, K. Wang, G. Xiao and B. Zou, Pressure regulating self-trapped states toward remarkable emission enhancement of zero-dimensional lead-free halides nanocrystals, *Small*, 2023, **19**, 2300455.
- 33 T. Geng, Y. Shi, Z. Liu, D. Zhao, Z. Ma, K. Wang, Q. Dong, G. Xiao and B. Zou, Pressure-induced emission from all-Inorganic two-Dimensional vacancy-ordered lead-free metal halide perovskite nanocrystals, *J. Phys. Chem. Lett.*, 2022, **13**, 11837–11843.
- 34 A. Devamanoharan, V. Venkatachalapathy, V. Veerapandy and P. Vajeeston, Investigating stable low-energy Gallium Oxide (Ga<sub>2</sub>O<sub>3</sub>) polytypes: Insights into electronic and optical properties from first principles, *ACS Omega*, 2024, **9**, 16207–16220.
- 35 S. Yoshioka, H. Hayashi, A. Kuwabara, F. Oba, K. Matsunaga and I. Tanaka, Structures and energetics of Ga<sub>2</sub>O<sub>3</sub> polymorphs, *J. Phys.: Condens. Matter*, 2007, **19**, 346211.
- 36 M. Hegde, T. Wang, Z. L. Miskovic and P. V. Radovanovic, Origin of size-dependent photoluminescence decay dynamics in colloidal  $\gamma$ -Ga<sub>2</sub>O<sub>3</sub> nanocrystals, *Appl. Phys. Lett.*, 2012, **100**, 141903.
- 37 P. Lv, D. Zhao, Z. Ma, M. Cong, Y. Sui, G. Xiao and B. Zou, Pressure-Modulated Interface Engineering toward Realizing Core@Shell Configuration Transition, *Nano Lett.*, 2023, **23**, 11982–11988.
- 38 I. Chatratin, F. P. Sabino, P. Reunchan, S. Limpijumng, J. B. Varley, C. G. Van de Walle and A. Janotti, Role of point defects in the electrical and optical properties of In<sub>2</sub>O<sub>3</sub>, *Phys. Rev. Mater.*, 2019, **3**, 074604.
- 39 H. Wu, Z. Wang and H. Fan, Stress-induced nanoparticle crystallization, *J. Am. Chem. Soc.*, 2014, **136**, 7634–7636.
- 40 P. Lv, Z. Ma, J. Ning, G. Xiao and B. Zou, Identification of defect origin and white-light emission tuning of chalcogenide quantum dots through pressure engineering, *CCS Chem.*, 2024, DOI: [10.31635/ccschem.024.202403971](https://doi.org/10.31635/ccschem.024.202403971).
- 41 A. Liang, R. Turnbull, C. Popescu, I. Fernandez-Guillen, R. Abargues, P. P. Boix and D. Errandonea, Pressure-induced phase transition versus amorphization in hybrid methylammonium lead bromide perovskite, *J. Phys. Chem. C*, 2023, **127**, 12821–12826.

